PERGAMON

Corrosion Science 43 (2001) 1227–1243

CORROSION SCIENCE

www.elsevier.com/locate/corsci

The corrosion behavior of scandium alloyed Al 5052 in neutral sodium chloride solution

Zaki Ahmad *, Anwar Ul-Hamid, Abdul-Aleem B.J.

Department of Mechanical Engineering, King Fahd University of Petroleum and Minerals, Dhahran 31261, Saudi Arabia

Received 28 June 1999; accepted 5 September 2000

Abstract

Alloying with scandium has a strong influence on the strengthening and weight saving characteristics of Al–2.5Mg alloys. Scandium addition (0.1–0.3 wt.%) to Al–2.5Mg alloys does not introduce any appreciable loss in their resistance to corrosion in 3.5 wt.% NaCl. The corrosion behavior of these alloys is not significantly affected by age hardening. Because of a unique combination of outstanding mechanical properties and a good resistance to corrosion Al–Mg alloys containing scandium represent a major improvement over the more familiar Al–Mg alloys.

Keywords: Corrosion; Al–Mg–Sc; Age-hardening; Microstructure; Pitting potential; Polarization

1. Introduction

The quest for high performance aluminum alloys has led to the emergence of new alloys such as Al–Be, Al–Li, Al metal matrix composites (MMCs) and powder metallurgy 7xxx and 2xxx series alloys. The family of Al–Li alloys offers the potential for weight savings in aircraft structures due to density reduction and stiffness improvement [1,2]. An alternate to lithium is magnesium, a strong solid solution strengthener, however, it has not been possible to produce competitive Al–Mg alloys that would match the level of strength, despite significant density reductions.

* Corresponding author. Tel.: +96-63-860-2540; fax: +96-63-860-2949.
E-mail address: ahmadz@kfupm.edu.sa (Z. Ahmad).

0010-938X/01/$ - see front matter
PII: S0010-938X(00)00147-5

Scandium has a special significance as it exceeds the strengthening action of all alloying elements (Mg, Cu, Zn, Si, Mn, etc.) in aluminum alloys [3,4]. An Al–Mg alloy containing 0.3 wt.% Sc showed a yield strength of 300 MPa, nearly double the strength of scandium-free alloys [5]. The attractive combination of properties is brought about by the Al_3Sc precipitate that is formed from super-saturated solution at elevated temperatures [6]. The strengthening effect appears only with hypereutectic Sc content (0.5–0.6 wt.%). However, the addition of zirconium to scandium makes it possible to obtain the same properties with a lesser scandium content (0.1–0.15 wt.%) [7]. The existing plethora of interest in Al–Mg–Sc alloys is centered around an excellent combination of physical and mechanical properties without any recourse to its service performance in corrosive environment. It is therefore of prime interest to evaluate the corrosion performance of Al–Mg–Sc alloys. Preliminary investigations were therefore undertaken to study the corrosion behavior of alloy 5052 containing scandium additions in 3.5 wt.% of sodium chloride. The corrosion behavior of these alloys has not been previously investigated.

2. Experimental methods

Aluminum alloys 5052 with 0.1 to 0.3 wt.% Sc additions were made by induction melting in a recrystallized alumina crucible under an argon atmosphere. Alloying with scandium powder was achieved in accordance with the guidelines of Leicht Metall, [1] Germany. The scandium powder was covered by a foil of pure aluminum to protect it from air contact and dipped in a melt covered by argon. The alloy was chill cast in a copper mold. The samples obtained from the alloys were termed as F tempers. Selected samples were aged in an oil bath for 10, 10^2, 10^3 and 10^4 min. They were solutionized for 1 h at 480°C prior to aging at 290°C.

The nominal compositions of Al–Mg–Sc alloys and other selected aluminum alloys mentioned in this work are given in Table 1.

Alloy without scandium is designated as alloy 1 whereas alloys containing scandium in concentrations ranging from 0.1 to 0.3 wt.% are designated as alloys 2, 3 and 4 respectively.

3. Specimen preparation

Specimens measuring 15 mm in diameter were used for electrochemical investigation and weight loss studies. They were polished with 320, 400 and 600 μm SiC paper using demineralized water as lubricant. Final polishing was done with a 6 μm diamond paste. The specimens were washed with demineralized water, rinsed with acetone and dried for 12 h before use.

[1] Leicht Metall – Kimpetenzzentrum, Ranshofen, Postfach 26, A-5282, Austria.

Table 1
Nominal composition of aluminum alloys

Alloy type	Si	Fe	Cu	Mn	Mg	Cr	Zn	Ti	Sc	Zr	Balance
6061	0.6	–	0.27	1.0	1.0	0.1	0.25	0.1	–	–	Al
5052	0.25	0.40	0.1	0.01	2.5	0.15	0.1	0.94	–	–	Al
6013	0.6	0.5	1.0	0.8	0.8	0.1	0.25	0.1	–	–	Al
Al–2.5Mg–0.1Sc	0.25	0.40	0.1	0.01	2.5	0.15	0.1	0.94	0.1	0.9	Al
Al–2.5Mg–0.15Sc	0.25	0.40	0.1	0.01	2.5	0.15	0.1	0.94	0.15	0.9	Al
Al–2.5Mg–0.30Sc	0.25	0.40	0.1	0.01	2.5	0.15	0.1	0.94	0.30	0.9	Al

4. Experimental procedure

4.1. Weight loss studies

The rate of corrosion after selected periods of exposure was determined by standard weight loss method in accordance with ASTM G31-72 practice [8]. Specimens in quadruplicate were used.

4.2. Polarization measurements

All potentiodynamic polarization measurements were made in accordance with ASTM standard practice G5-87 [9] (standard practice for cyclic potentiodynamic polarization measurement).

The specimen is polarized for 1 h at −1200 mV with respect to a saturated calomel electrode in 3.5 wt.% NaCl. Polarization is commenced at a scan rate of 10 mV/min and continued in the noble direction until a sharp rise in the current, indicating the onset of pitting, is observed. The scan is reversed after it reaches the pitting potential and continued in the reverse direction until the current drops to a very small value. The protection potential (E_{pp}) is determined by the intersection of the reverse anodic polarization curve with the forward anodic polarization curve.

4.3. Microstructure examination

The surface morphology of the corroded samples was investigated by a scanning electron microscope. Microanalytical studies were conducted by an EDS system with X-ray mapping capabilities. Specimens were ground with 300, 400 and 600 grit size abrasive and polished with a 6 μm diamond paste. Specimens were thinned to 120 μm and put in a dimpler to obtain a thickness of 60 μm. For final thinning a 10 kV ion beam with high-energy gun at 1° from the surface was applied on both sides until perforation occurred.

5. Results and discussion

5.1. Mechanical properties

The mechanical properties of Al–Mg–Sc alloys are primarily affected by alloying elements of Mg, Zr, Ti and Sc. Magnesium increases the strength by 35 MPa for each addition of 1% [10]. Zirconium inhibits re-crystallization and acts as a strengthener. Scandium increases the strength by 55 MPa for each 0.1% increment [7]. Titanium is used as a grain refiner.

Limited studies on the mechanical properties of the four alloys were conducted. Bars measuring 0.25×3 in.^{2} were extruded from 5 in. diameter billets and subjected to tests in accordance with ASTM testing procedures [8,9]. The results are summarized in Table 2. The results establish the useful effect of Sc as a potent strengthener. It has been shown by other investigators that scandium addition provides the much needed thermal stability to high performance aluminum alloys which otherwise suffer from degradation of mechanical properties at elevated temperatures [11].

5.2. Microstructure and surface morphology

Microstructural variations play a dominant role in the corrosion of Al–Mg–Sc alloys. Fig. 1 shows the microstructure of Al–Mg–0.15Sc alloy after age hardening for 10^4 min. The rectangular precipitate constitutes mainly Fe, Sc and Al as shown by EDS analysis. Fig. 2 shows another precipitate (white) containing Ti, Sc and Al. The distribution of fine precipitates of Al_3Sc and dislocations are shown in TEM micrograph (Fig. 3). The pinning down of the grain boundaries by Al_3Sc precipitates is shown in Fig. 4. The above observations are supported by other investigators who conducted similar TEM studies [6,11,12].

5.3. Corrosion studies

The corrosion studies were divided in two parts: weight loss studies and electrochemical studies. The weight loss studies conducted in 3.5 wt.% NaCl showed that the corrosion rate decreased with increased exposure period. For instance, the corrosion rate of alloy containing 0.1 wt.% Sc decreased from 2.4 to 1.44 mdd (0.038 to

Table 2
Mechanical properties of Al–Mg–Sc alloys

No.	Alloy designation	Yield strength (ksi)	Ultimate tensile strength (ksi)	Elongation (%)
1	Al–2.5Mg	23	31	14
2	Al–2.5Mg–0.1Sc	29.3	38.5	10.0
3	Al–2.5Mg–0.15Sc	31.3	39.5	9.5
4	Al–2.5Mg–0.30Sc	37	41.5	9.0

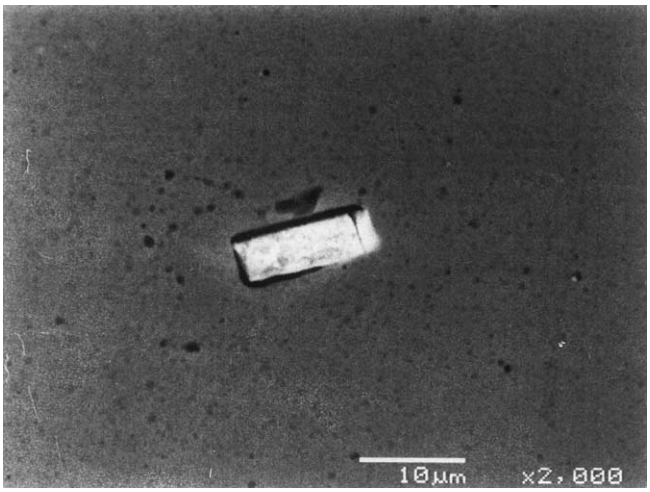

Fig. 1. SEM image of Al–2.5Mg–0.15Sc alloy after age hardening for 10^4 min at 260°C. The precipitate shows the presence of Fe, Sc and Al.

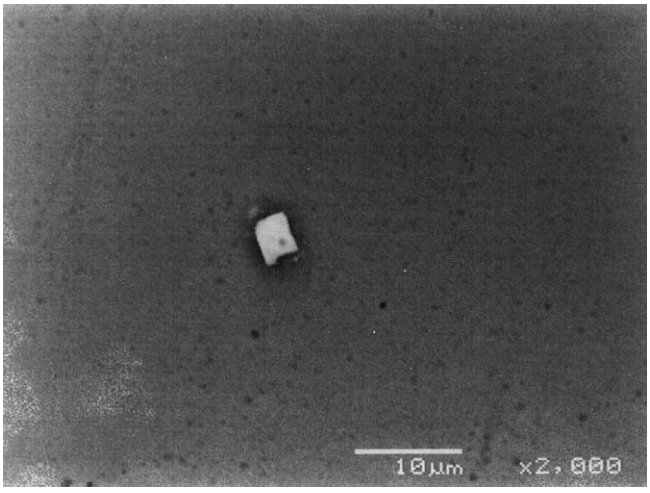

Fig. 2. SEM image of Al–2.5Mg–0.15Sc alloy showing the precipitate enriched in Ti, Al and Sc.

0.023 mm/year) after an exposure period of 800 h. This trend is inherent in Al–Mg alloys and it is attributed to the slow build up of a duplex protective film of either bayerite (β-$Al_2O_3 \cdot 3H_2O$) or boehmite (γ-$Al_2O_3 \cdot H_2O$). A steady state is reached when the rate of oxide formation at the aluminum oxide interface just equals the rate of oxide dissolution at the oxide solution interface [13]. The nature of duplex film has been the subject of intensive research in the past [13,14]. The surface of alloy 2 was

Fig. 3. TEM micrograph of Al–2.5Mg–0.3Sc alloy showing a high dislocation density at the subgrain boundaries.

identified to be covered by a film of boehmite after drying as shown by Fig. 5. The corrosion rate of alloys containing 0.1–0.3 wt.% Sc obtained by immersion in 3.5 wt.% of NaCl for 400 h are given in Table 3. There is not an appreciable increase in the corrosion rate on addition of 0.1 to 0.15 wt.% Sc. The reason for a slight decrease in the corrosion rate on addition of 0.3 wt.% Sc is not clearly understood. The corrosion rate of the alloy with different levels of scandium obtained by polarization studies is shown in Tables 4 and 5. Selected polarization curves are shown in Fig. 6. It is observed from Tables 4 and 5 that age hardening does not have a pronounced effect on the corrosion resistance of the alloys. Limited studies with 0.3 wt.% Sc showed the same behavior.

The corrosion rate is increased slightly by adding 0.1–0.15 wt.% Sc, however, the increase is not significant. Scandium addition does not appear to increase the corrosion rate as other elements in conventional aluminum alloys as shown by the typical corrosion rates of alloys 5050, 5052, 6013 and 6061 in similar environments (Table 6) in 3.5 wt.% NaCl. It can be observed that the corrosion rates are either equal or better than the corrosion rates of more familiar aluminum alloys in similar environment.

Fig. 4. TEM micrograph of Al–2.5Mg–0.3Sc alloy after 10^4 min at 260°C showing the pinning down of subgrain boundary by Al_3Sc precipitate.

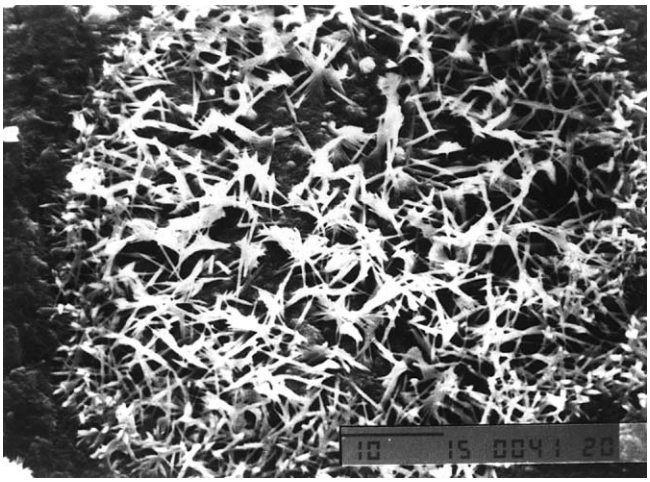

Fig. 5. SEM image showing the surface of Al–2.5Mg–0.15Sc covered by crystalline boehmite after drying.

5.3.1. Age-hardening

The effect of aging treatment on the pitting potential of the alloys is shown in Table 7. The effect of age hardening on the corrosion rates is not very significant as shown in the combined polarization diagrams (Fig. 7). The pitting potentials are not

Table 3
Corrosion rate of Al–Mg–Sc alloys in 3.5 wt.% of NaCl obtained by weight loss technique (after 400 h)

Alloy	Corrosion rate	
	mm/year	mdd[a]
Al–2.5Mg	0.023	1.477
Al–2.5Mg–0.1Sc	0.031	1.980
Al–2.5Mg–0.15Sc	0.046	2.914
Al–2.5Mg–0.30Sc	0.038	2.46

[a] mdd — milligrams per square decimeter per day.

Table 4
Summary of results of polarization resistance measurement of Al–Mg–Sc alloy in 3.5 wt.% NaCl

Sample type and hardening time	$E(I=0)$ (mV)	R_p (Ω-cm^2)	I (A/cm^2)	Corrosion rate	
				mm/year	mpy[a]
Al–2.5Mg–0Sc (0 min)	−595.1	1.15E+04	4.57E−06	0.050	1.96
Al–2.5Mg–0.10Sc (0 min)	−878.1	7.40E+03	7.15E−06	0.038	1.505
Al–2.5Mg–0.15Sc (0 min)	−900.9	9.17E+03	8.99E−06	0.054	2.132
Al–2.5Mg–0.30Sc (0 min)	−697.3	2.19E+04	6.19E−06	0.054	2.132
Al–Mg–0.10Sc (10 min)	−876.2	2.90E+03	1.09E−06	0.039	1.541
Al–Mg–0.10Sc (10^2 min)	−827.7	7.70E+03	4.33E−06	0.050	1.981
Al–Mg–0.10Sc (10^4 min)	−862.6	7.41E+03	5.89E−06	0.064	2.53

[a] mpy — mils per year.

Table 5
Summary of results of potentiodynamic polarization (TAFEL analysis) of Al–Mg–Sc alloy in 3.5 wt.% NaCl

Sample type and hardening time	$E(I=0)$ (mV)	ATC[a] (mV/decade)	CTC[b] (mV/decade)	I (A/cm^2)	Corrosion rate	
					mm/year	mpy
Al–2.5Mg–0Sc (0 min)	−885.5	150.9	596.6	4.51E−06	0.050	1.936
Al–2.5Mg–0.10Sc (0 min)	−878.1	202.1	306.2	6.66E−06	0.073	2.857
Al–2.5Mg–0.15Sc (0 min)	−906.7	363.6	398.1	5.51E−06	0.060	2.366
Al–2.5Mg–0.30Sc (0 min)	−631.4	992.5	870.2	4.31E−06	0.030	1.184
Al–Mg–0.10Sc (10 min)	−877.3	126.9	176	4.66E−06	0.049	1.917
Al–Mg–0.10Sc (10^2 min)	−786.8	92.3	460.3	6.03E−06	0.070	2.756
Al–Mg–0.10Sc (10^4 min)	−838	329.8	329.8	5.30E−06	0.068	2.69

[a] ATC – anodic Tafel constant.
[b] CTC – cathodic Tafel constant.

significantly affected as shown by the typical behavior of alloy 2 (Table 7). Microhardness measurements revealed that Al–2.5Mg alloys containing 0.1–0.3 wt.% Sc are not very responsive to age hardening. This is illustrated by Fig. 8 which shows

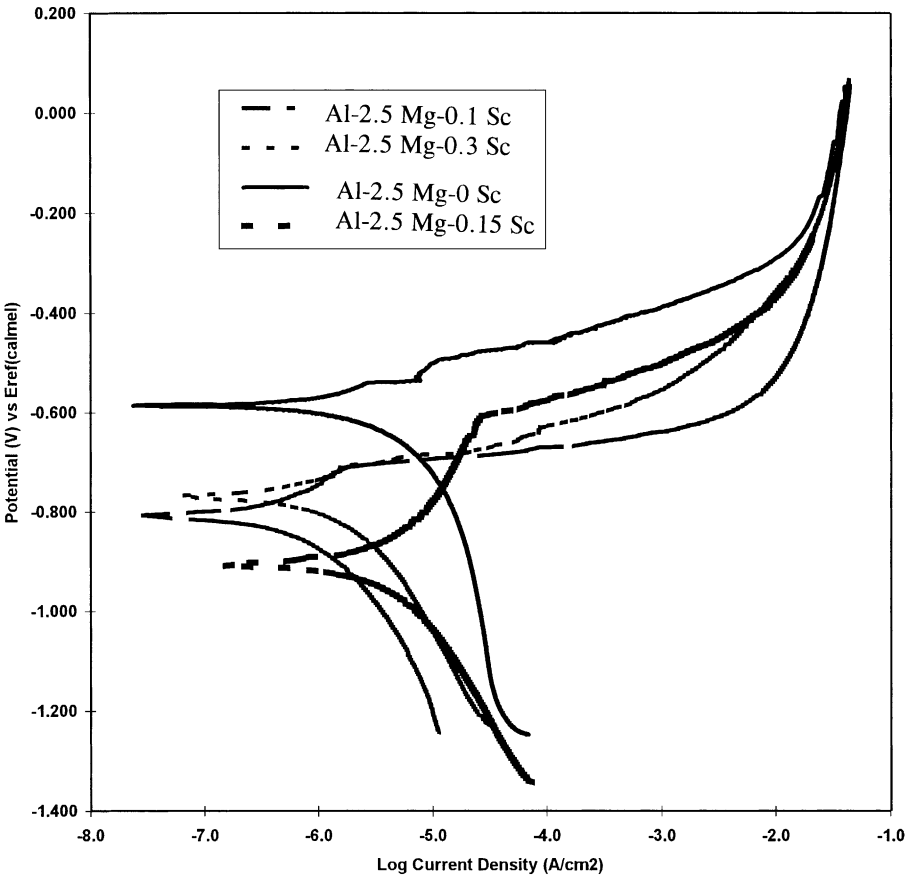

Fig. 6. Combined potentiodynamic polarization diagram of Al–2.5Mg–Sc(0.1–0.3) alloys in 3.5 wt.% of NaCl.

Table 6
Corrosion rates of commercial aluminum alloys

Alloy designation	Corrosion rate (mm/year)
6061	0.109 [15]
5052 (0 Zr)	0.071 [16]
3023	0.075 [16]
6063	0.109 [16]
6013	0.089 [17]

the effect of aging time on micro-hardness. Further work with high concentrations of Sc (0.3–0.6 wt.%) is in progress.

Pitting studies were conducted by the well-known ASTM cyclic polarization techniques. A typical cyclic polarization diagram is shown in Fig. 9. The diagram

Table 7
Pitting potential (E_p) and protection potential (E_{pp}) of Al–2.5Mg–0.1Sc alloy in 3.5 wt.% NaCl age hardened for 10, 10^2 and 10^3 min

Sample	E_p (V)	E_{pp} (V)	E_{corr} (V)
As fabricated	−0.761	−0.826	−0.831
10 min	−0.638	−0.808	−0.755
10^2 min	−0.735	−0.825	−0.812
10^3 min	−0.743	−0.832	−0.849

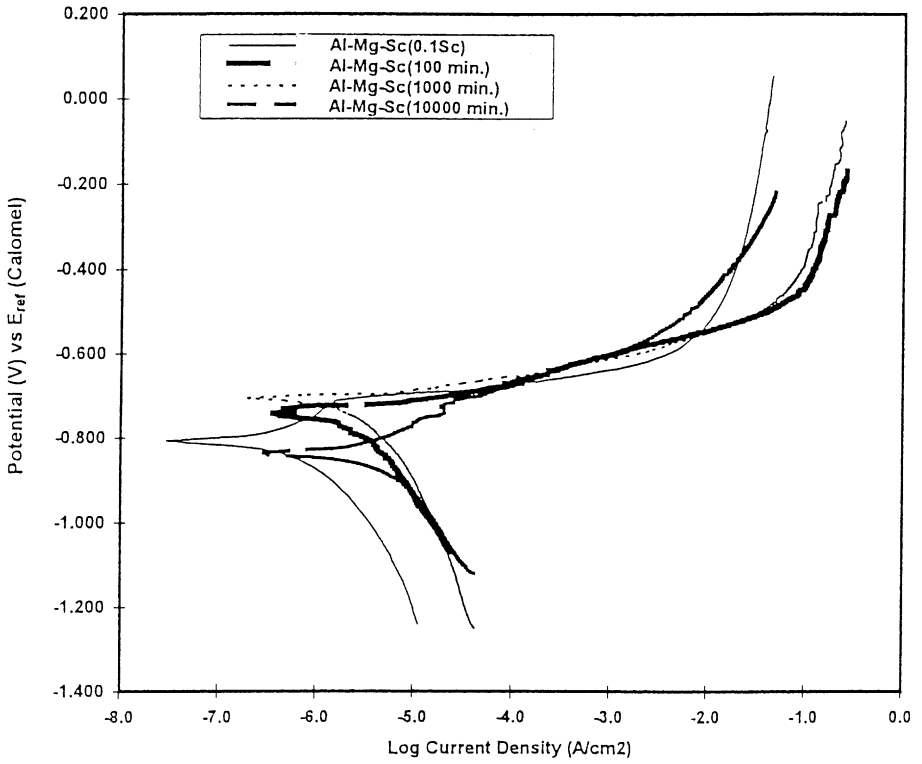

Fig. 7. Combined potentiodynamic polarization diagram of Al–2.5Mg–0.1Sc alloy showing the effect of age hardening.

shows pitting potential (E_p), protection potential (E_{pp}) and corrosion potential (E_{corr}). Pitting potential (E_p) is the reproducible experimental measurement characteristic of pit initiation. Protection potential (E_{pp}) exists between the oxide covered metal and electrolyte. Pits do not initiate or propagate below E_{pp}. As the pitting potential (E_p) increases pitting susceptibility decreases. The pitting potential (E_p) of the four alloys is shown in Table 8.

Smaller Sc content as shown by alloys 1 and 2 does not affect the pitting potential. The pitting potential tends to become more negative with increasing Sc content as

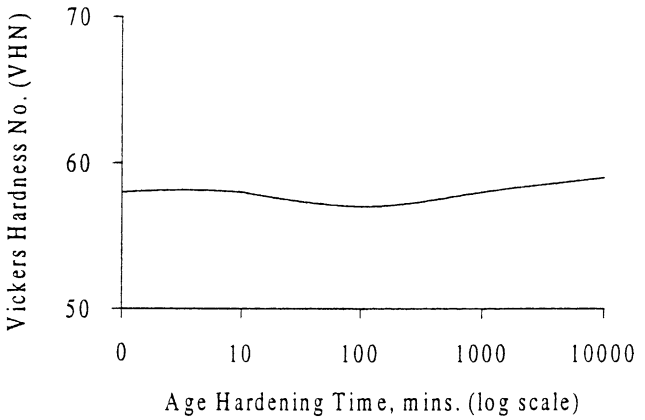

Fig. 8. Vickers hardness vs age hardening time (min) for Al–2.5Mg–0.15Sc alloy.

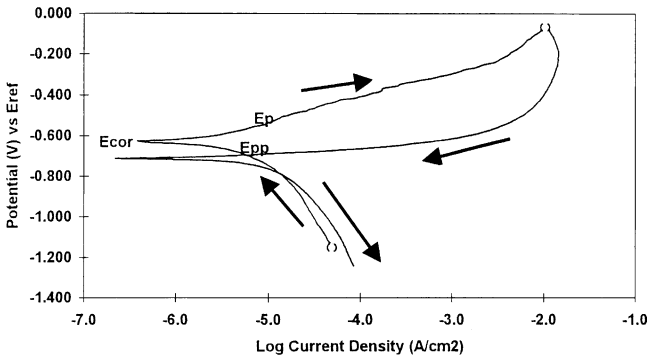

Fig. 9. Potential cyclic polarization diagram for Al–2.5Mg–0.15Sc in 3.5 wt.% NaCl.

Table 8
Pitting potential (E_p) and protection potential (E_{pp}) of Al–2.5Mg–Sc(0–0.3) alloy in 3.5 wt.% NaCl

Alloy	E_p (V)	E_{pp} (V)	E_{corr} (V)
Al–2.5Mg–0Sc	−0.521	−0.697	−0.643
Al–2.5Mg–0.1Sc	−0.578	−0.713	−0.659
Al–2.5Mg–0.15Sc	−0.518	−0.694	−0.628
Al–2.5Mg–0.30Sc	−0.670	−0.729	−0.742

shown by alloy 4. A more negative potential signifies an easier breakdown and initiation of pits [16]. The pitting potential exhibited by the alloys meet the criteria that E_{corr} be more negative to E_p for good pitting performance. The pitting potentials of Al–Mg–Sc alloys 2, 3 and 4 are positive to E_{corr} in all instances. The pitting

Table 9
Selected E_p values of some selected aluminum alloys in 3.5 wt.% NaCl

Alloy designation	E_p V vs SCE	Reference
Al 6061	−0.669	[17]
Al 6013	−0.688	[17]
Al 2024	−0.540	[18]
Al 5456	−0.695	[18]

potentials of some selected aluminum alloys which are known to exhibit a good resistance to pitting in 3.5 wt.% NaCl are given in Table 9 for comparison.

It is observed that the pitting potential of alloys 2, 3 and 4 are at least equal to or more positive compared to the pitting potential of alloys listed in Table 9.

The pitting morphology on Al–Mg–Sc alloys as observed by SEM is shown by Figs. 10–12. Irregular shaped crystallographic pits are observed on the surface of alloys. The surface morphology tends to alter with an increase in Sc (0.3 Sc) content. Irregular crystallographic pits as well as some hemispherical pits can be observed on alloy 4 (0.3 Sc) (Fig. 12). The pit depths of the four alloys investigated are shown in Table 10.

The pits on alloy surface 2, 3 and 4 are shallow and smaller compared to alloy 1 (5052–0 Sc, Fig. 13). The maximum pit depths compare favorably with the pitting depths observed in conventional alloys 6061 and 6013 determined by the author. Results of the investigation show that Al–Mg–Sc alloys offer a good resistance to pitting in 3.5 wt.% NaCl. It has been shown by TEM studies described earlier that Al_3Sc precipitates are of a very small size (8–10 nm) and they are coherent with the

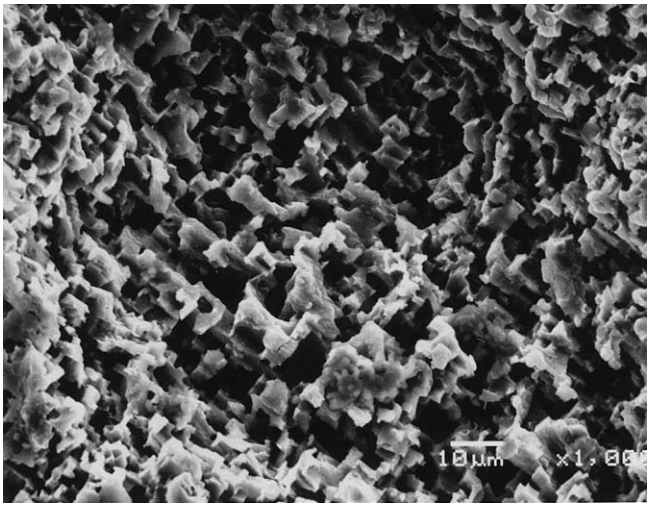

Fig. 10. Photomicrograph of Al–2.5Mg–0.1Sc showing crystallographic pitting (100×).

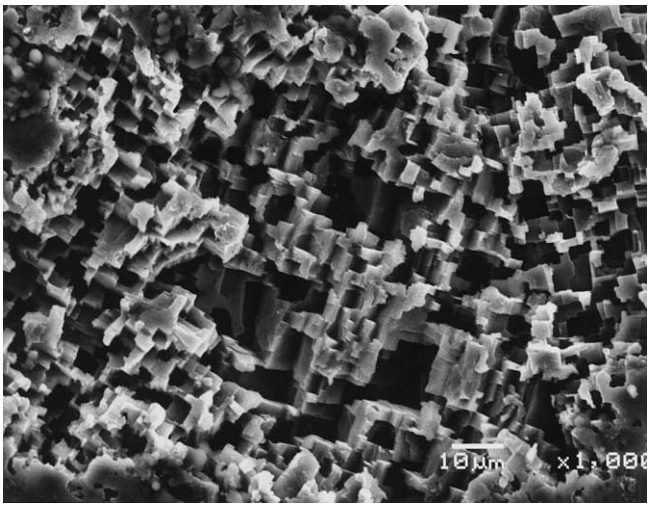

Fig. 11. Photomicrograph of Al–2.5Mg–0.15Sc showing crystallographic pitting (100×).

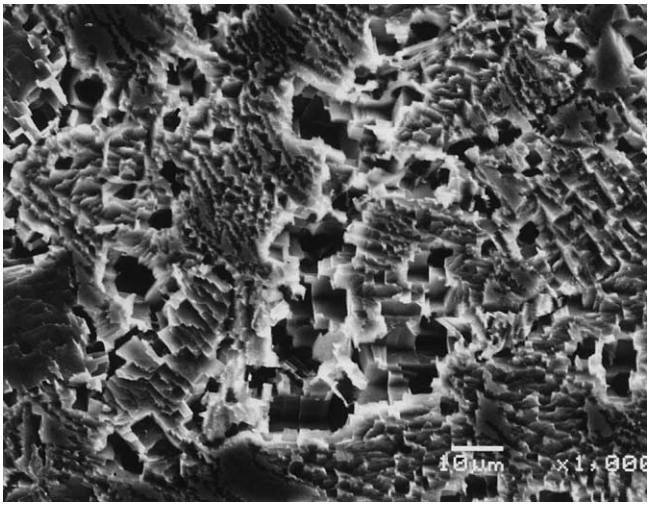

Fig. 12. Photomicrograph of Al–2.5Mg–0.15Sc showing hemispherical pits (100×).

Table 10
Pit depths of Al–Mg–Sc alloys in 3.5 wt.% NaCl

Alloy	Average pit depth (μm)	Maximum pit depth (μm)
1	95	182
2	55	110
3	70	108
4	18	30

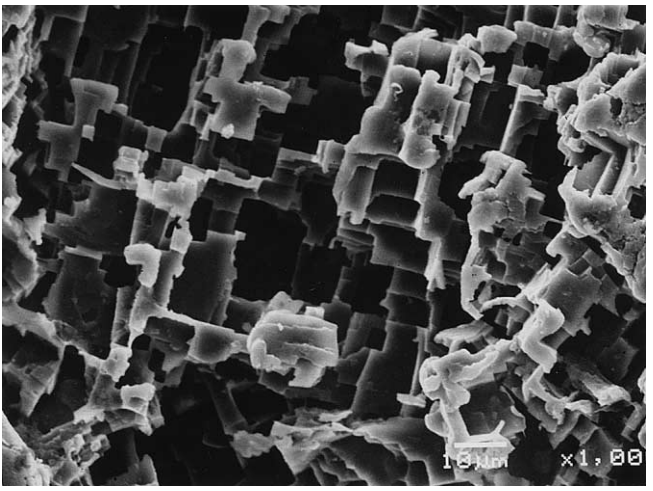

Fig. 13. Photomicrograph of Al–2.5Mg–0Sc showing deep crystallographic pits (100×). A highly faceted structure is observed.

matrix [11]. One would expect fewer flaws and lesser discontinuities at the precipitate/oxide/electrolyte interface in Al–Mg–Sc alloys compared to alloys 2024, 6061 and 6013 which contain large size precipitates of $CuAl_2$ and $CuMgAl_2$. It has been shown that an increase in size of $CuAl_2$ or $CuMgAl_2$ precipitate decreased the pitting potential and increased the susceptibility to pitting. It has been shown that larger number of intermetallics in alloy 5456 provide active sites for intensive pitting [19]. The presence of $CuMgAl_2$ intermetallic in AA 2124 caused extensive pitting because of inherent discontinuities created at precipitate/oxide/electrolyte interface [20]. The pitting potential (E_p) and corrosion potential (E_{corr}) become more negative with an increase in the precipitate size. The pitting potential of Al–2.5Mg–Sc alloys is slightly more positive than the pitting potentials of aluminum alloys shown in Table 9 which suggests that the precipitate size is not of a sufficient size to influence the pitting potential.

More microanalytical studies would be needed to establish the role of Al_3Sc precipitate in pitting morphology of the alloys. The relationship between microstructure and pitting morphology has not been fully established even in conventional aluminum alloys. The consensus of investigators is that the pitting morphology of aluminum alloys depends upon the electrochemical behavior of matrix, nature of intermetallics, their composition and size of homogeneity of distribution. The intermetallics provide active sites for pit initiation. The breakdown of oxide film around the pits is shown in Fig. 14. Pits are covered by a white gelatinous product of $Al(OH)_3$ which solidifies upon drying. The $Al(OH)_3$ gel has to be removed by an orthophosphoric chromic acid mixture to observe pits. Covering of pits by $Al(OH)_3$ has been referred to as *Corrosion Chimney* in the literature [21]. The gelatinous $Al(OH)_3$ which is pumped out by pits dries up eventually and cracks in

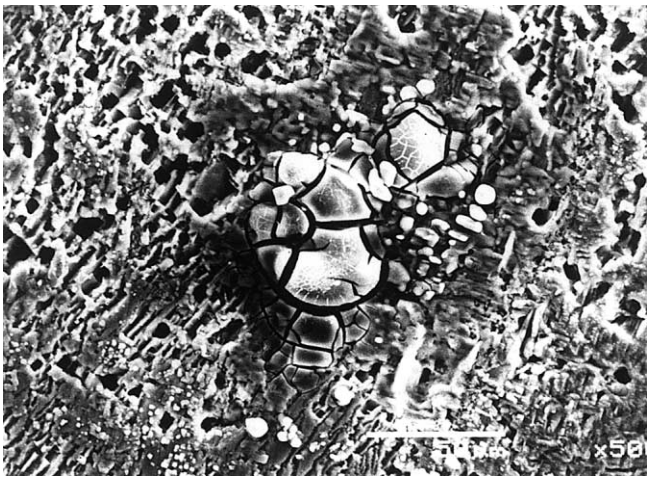

Fig. 14. Photomicrograph of Al–2.5Mg–0.15Sc showing covering of pits by gelatinous $Al(OH)_3$.

the form of mud-cracking (Fig. 15). It is, however, not an artifact of localized corrosion.

The investigations conducted have shown that Al–Mg–Sc alloys show a good resistance to localized corrosion. The new data on corrosion coupled with the outstanding mechanical and physical properties of the alloys mentioned earlier shows that these alloys are highly promising future materials. However, intensive work on the microstructure related corrosion studies is needed to fully exploit the role of scandium in aluminum magnesium alloys.

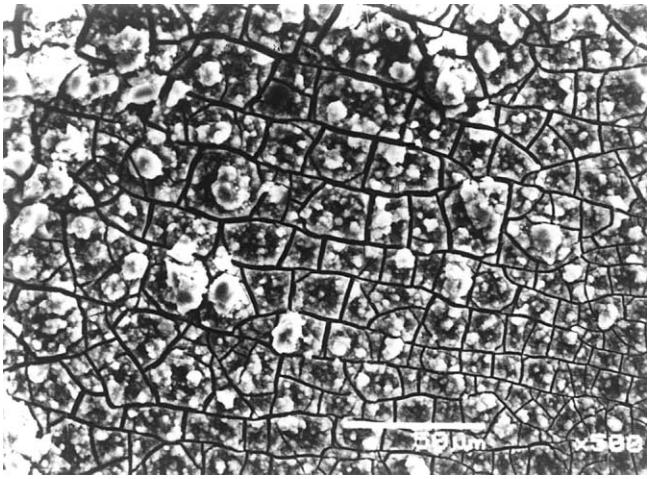

Fig. 15. Photomicrograph of Al–2.5Mg–0.3Sc showing mud cracking (100×).

6. Conclusions

On the basis of the results obtained from the investigations, the following are the main conclusions:

1. Addition of 0.1–0.3 wt.% scandium introduces a relatively high level of strength in Al–Mg alloys as shown by the improvements in mechanical properties.
2. Precipitates of Al_3Sc present in Al–2.5Mg–Sc alloys affect the corrosion behavior of these alloys. These precipitates are also responsible for the strengthening of the alloys as shown by the pinning down of the grain boundaries.
3. Scandium addition (0.1–0.3 wt.%) does not introduce any appreciable increase in the corrosion rate of Al–Mg alloys. Al–2.5Mg–Sc (0.1–0.3) alloys offer a better resistance to corrosion as compared to that offered by important commercial aluminum alloys such as 5052, 6061, 6013, 5456, etc.
4. The Al–2.5Mg–Sc alloys exhibit irregular crystallographic pits with small pitting depths. The pitting potentials of the alloys are observed to be more positive compared to commercial Al–Mg alloys.
5. Because of a unique combination of outstanding mechanical properties and a good resistance to corrosion, Al–2.5Mg–Sc (0.1–0.3) alloys represent a major improvement over the more familiar Al–Mg alloys.

Acknowledgements

The authors are grateful to Dr. Timothy Langen of Ashurst Government Services for providing some of the materials and for his valuable technical cooperation. The authors acknowledge the experimental work conducted by Mr. M. Saleh, Engineer, Corrosion Laboratory at KFUPM. We are also thankful to Mr. Abdul-Rashid I. Mohammed for his assistance in metallographic sample preparation. The support provided by KFUPM is highly appreciated.

References

[1] L.A. Willey, US Patent 3619181, 1975.
[2] M.E. Drits, S.V. Pavellenko, L.S. Torpova, Sov. Phy. Doki 26 (1981) 344.
[3] M.E. Drits, J. Dutekiewicz, L.S. Torpova, Cryst. Technol. 24 (1984) 1325.
[4] V.I. Elagin, V.V. Zakharov, T.D. Rostoras, Mater. Sci. Heat Treatment 34 (1992) 37.
[5] B.A. Parker, Z.F. Zhou, P. Nolle, J. Mater. Sci. 30 (1995) 452.
[6] R.R. Sawtell, C.L. Jensen, Metall. Trans. 21A (1990) 421.
[7] V.I. Elagin, V.V. Zakharov, T.D. Rostoras, Metallovedeniei Termicheskaya Obrabotka 1 (1992) 24.
[8] ASTM: Recommended Practice G31-72 (78) for Immersion Corrosion Testing of Metals, Annual Book of Standards, vols. 3 and 2, Part 10, 1998.
[9] ASTM: Recommended Practice G5-87 for Making Potentiostatic and Potentiodynamic Polarization Measurement, Annual Book of Standards, vols. 3 and 2, Part 10, 1998.
[10] Davis, R. Joseph (Ed.), Aluminum and Aluminum Alloys, ASM Specialty Handbook, ASME, 1996.
[11] S. Krause, et al. Phys. Stat. A311 (1994) 2861.

[12] N. Blake, M.A. Hopkins, J. Mater. Sci. 20 (1980) 311.
[13] R.K. Hart, Proc. Royal Soc. Lond. A236 (1956) 68.
[14] J.E. Draley, W.E. Ruther, Corrosion 12 (1956) 31.
[15] S.N. Bhatt, M.K. Surappa, J. Mater. Sci. 26 (1991) 4991.
[16] G. Venkateswaran, K.S. Venkateswaran, Proc. Int. Cong. Metallic Corros. 1987, p. 1587.
[17] Z. Ahmad, A.B.J. Aleem, KACST Project Final Report AR14-65, 1999.
[18] P.O. Trazskoma, Corrosion 46 (1990) 402.
[19] J.F. McIntyre, A.H. Lee, S.L. Golledge, R.K. Conrad, Corrosion 46 (1990) 11.
[20] J.F. McIntyre, A.H. Lee, S.L. Golledge, R.K Conrad, Technical Report, NSWC, TR 87-326, 1987.
[21] T.D. Burleigh, E. Ludwiczak, R.D. Peti, Corros. Sci. 51 (1995) 1.